

This is the peer reviewed version of the following article:

Anomalous random telegraph noise and temporary phenomena in resistive random access memory / Puglisi, Francesco Maria; Larcher, Luca; Padovani, Andrea; Pavan, Paolo. - In: SOLID-STATE ELECTRONICS. - ISSN 0038-1101. - 125:(2016), pp. 204-213. [10.1016/j.sse.2016.07.019]

Terms of use:

The terms and conditions for the reuse of this version of the manuscript are specified in the publishing policy. For all terms of use and more information see the publisher's website.

18/12/2025 19:42

Anomalous Random Telegraph Noise and Temporary Phenomena in Resistive Random Access Memory

Francesco Maria Puglisi¹, Luca Larcher^{2,3}, Andrea Padovani³, Paolo Pavan¹

¹DIEF, Università di Modena e Reggio Emilia, Via P. Vivarelli 10/1, 41125 – Modena (MO) - Italy

²DISMI, Università di Modena e Reggio Emilia, Via Amendola 2, 42122 – Reggio Emilia (RE) - Italy

³MDLab s.r.l., Località Grand Chemin 30, 11020 Saint-Christophe (AO), Italy

email: francescomaria.puglisi@unimore.it

Abstract— In this paper we present a comprehensive examination of the characteristics of complex Random Telegraph Noise (RTN) signals in Resistive Random Access Memory (RRAM) devices with TiN/Ti/HfO₂/TiN structure. Initially, the anomalous RTN (aRTN) is investigated through careful systematic experiment, dedicated characterization procedures, and physics-based simulations to gain insights into the physics of this phenomenon. The experimentally observed RTN parameters (amplitude of the current fluctuations, capture and emission times) are analyzed in different operating conditions. Anomalous behaviors are characterized and their statistical characteristics are evaluated. Physics-based simulations considering both the Coulomb interactions among different defects in the device and the possible existence of defects with metastable states are exploited to suggest a possible physical origin of aRTN. The same simulation framework is also shown to be able to predict other temporary phenomena related to RTN, such as the temporary change in RTN stochastic properties or the sudden and iterative random appearing and vanishing of RTN fluctuations always exhibiting the same statistical characteristics. Results highlight the central role of the electrostatic interactions among individual defects and the trapped charge in describing RTN and related phenomena.

Keywords - Random Telegraph Noise (RTN), Anomalous RTN, RRAM, Resistive switching, Trap-Assisted Tunneling (TAT).

I. INTRODUCTION

In the vast landscape of emerging memory devices, the Resistive Random Access Memory (RRAM) is among the most promising options to become the near-future memory device of choice for both embedded and stand-alone applications. Their excellent characteristics such as fast, low-power switching and CMOS-compatibility [1-2] configure RRAM as one of the best candidates for flash memories replacement. Nevertheless, reliability and variability problems [3-4] are hampering the full industrial exploitation of RRAM devices. Particularly, Random Telegraph Noise (RTN), i.e. the sudden shift of current among discrete values observed during readout operations, affects the reliability of these memory devices, as it could result in the failure of the readout operation, i.e. erratic bit detection [4-6]. RTN is generally associated with trapping and de-trapping of charge carriers into/from defects in the device structure [5-6]. Although the typology of the defects triggering RTN has not been unambiguously identified yet, recent studies suggest that RTN could be the result of the activation and deactivation of oxygen vacancy defects (Vo), which assist charge transport [5-6]. However, the state-of-the-art comprehension of RTN and

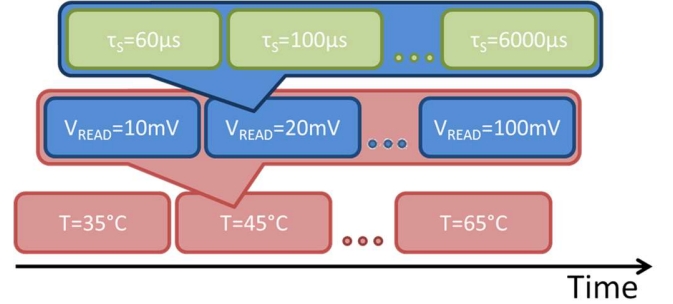


Figure 1. Schematic representation of the systematic experiment. Different consecutive RTN measurements are performed using different sampling times (green blocks), V_{READ} (blue blocks), and temperatures (red blocks).

related phenomena is quite incomplete: besides conventional RTN, also more bizarre signals have been detected, as the anomalous RTN (aRTN), i.e. RTN fluctuations appearing and disappearing over time in an iterative fashion [7], or RTN signals exhibiting temporary mutations of their statistical properties. The existence of these features further complicates the underlying physical picture and hinders its characterization, which is necessary to improve the reliability of these devices. In this paper, we exploit careful systematic experiment, dedicated characterization procedures, and comprehensive physics-based simulations to investigate aRTN behavior. The peculiar systematic experiment allows fully characterizing the aRTN signals in different operating conditions. A sophisticated data analysis technique is exploited to properly handle complex experimental data. Moreover, physics-based simulations able to reproduce multi-level RTN signals characteristics in different operating conditions are exploited to gain insights into the possible physical mechanisms responsible for the observed aRTN. The same physical framework is used to also predict the possible physical origin of other temporary phenomena related to RTN and detected in these devices, such as the temporary change in RTN stochastic properties, i.e. mutant RTN (mRTN) and the sudden and iterative random appearing and vanishing of RTN fluctuations, i.e. temporary RTN (tRTN).

II. DEVICES AND EXPERIMENTS

A. Device Details

TiN/Ti/HfO₂/TiN cross-bar RRAM devices in 1T-1R configuration are considered. The access transistor is used to both select the memory cell and to limit the current flow in the

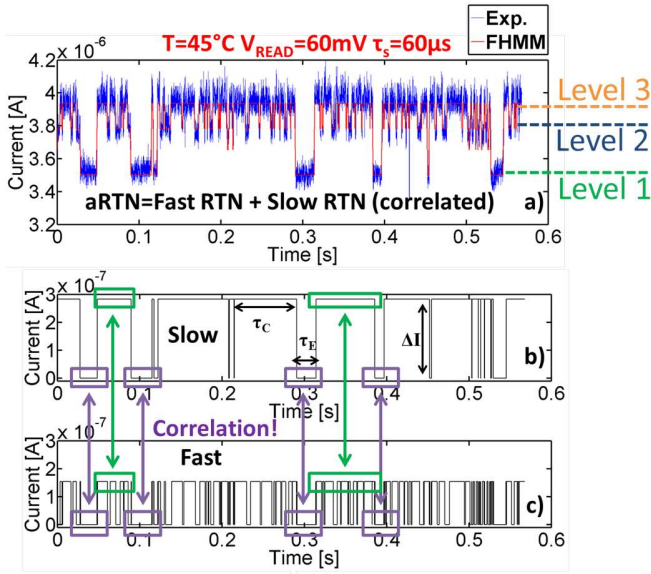


Figure 2. (a) Example of an aRTN signal, which exhibits three discrete current levels (Level 1 to Level 3) and is composed of a slow and a fast RTN component showing correlation. The fast component is only visible when the slow component is in the high-current state. (b,c) The aRTN signal in (a) is decomposed into separate two-level fluctuations. Correlation between the two components is shown (see violet boxes and arrows).

device by imposing the requested current compliance, preventing current overshoots to occur during the forming operation [8]. Devices with $100 \times 100 \text{ nm}^2$ area, 3.4nm Atomic Layer Deposition (ALD) HfO_2 , and 5nm Ti layer are investigated. The Ti film on top of the switching oxide layer determines some oxygen deficiency in the underlying ALD-grown HfO_2 , which has been proven to be crucial to achieve reliable resistive switching [9].

B. Experiments

After the preliminary forming operation (employing a current compliance $I_c=100\mu\text{A}$), we verify the correct behavior of the device under test, which shows bipolar filamentary switching as expected [9]. Then, we drive the device in High-Resistive State (HRS) performing a DC sweep reset operation using $V_{\text{RESET}}=-1\text{V}$. From the resulting I-V curve we estimate the conductive filament (CF) cross-section and the dielectric barrier thickness exploiting the compact model for HfO_2 RRAM devices in [10-11]. The device is now in the desired state for the RTN analysis, so henceforth it is not switched to any further extent. This implies we analyze the behavior of a single programmed bit in different operating conditions. The RTN current fluctuations in HRS are recorded in the time domain (I-t traces) applying a constant biasing voltage, V_{READ} . Since anomalous RTN signals may randomly appear and disappear, a careful design of experiment is required for a reliable characterization. Furthermore, RTN characteristics (amplitude of the RTN fluctuation, average capture and emission times) strongly vary with the operating conditions (i.e. applied voltage and temperature). Hence, different measurement settings (i.e. sampling and measurement times) may be required to accurately characterize anomalous RTN signals in different operating conditions. In our systematic experiment, schematically depicted in Fig. 1, characterization

and measurement conditions are automatically changed. Each green block in Fig. 1 represents a specific RTN measurement operation, which is completely defined by the sampling time, τ_s , the applied bias voltage, V_{READ} , and the temperature, T . Each measurement contains 10k points, i.e. the total measurement time is $T_{\text{meas}}=10\text{k} \cdot \tau_s$. Consecutive measurements are performed at different sampling times (ranging from $60\mu\text{s}$ to 6ms, Fig. 1) in the same operating conditions (voltage and temperature). This procedure (represented by blue blocks) is repeated at different voltages (from 10mV to 100mV, Fig. 1). This measurement cluster (represented by red blocks) is then repeated applying different temperatures (from 35°C up to 65°C , Fig. 1). The choice of the temperature, voltage, and sampling time ranges used in this experiment allows accurately observing RTN over time in different operating conditions while preventing the device resistive state from switching. Moreover, the accuracy of the RTN parameters estimation is improved by the availability of data recorded at different sampling times which allows optimizing the trade-off between accuracy and resolution during the RTN data analysis. The quantitative assessment of RTN parameters and their extraction from experimental multi-level RTN traces is achieved using a custom-developed software tool implementing the Factorial Hidden Markov Model (FHMM) algorithm [12-13]. This powerful tool allows decomposing multi-level RTN signals into many independent two-level signals, each attributed to the activation and deactivation of an individual defect. This allows correctly assessing the statistical characteristics of every individual defect contributing to the observed multi-level RTN [12-13].

C. Simulations

Simulations of I-t traces are performed using the MDLab simulations suite [14], accounting for the lattice relaxation, i.e. electron-phonon interaction, both trap-assisted and directing tunneling, charge transport through defects sub-bands, 3D temperature and potential maps (including the effect of trapped charge), metastable states, transitions among different defect charge states, and offers the possibility of performing kinetic Monte-Carlo (kMC) simulations. Moreover, it is possible to include the effects of defects generation (Hf-O bond breakage), recombination among complementary defect species, and defects drift-diffusion. Additional details about the simulation environment may be found in [14-16].

III. ANOMALOUS RTN: RESULTS AND DISCUSSION

The experiment reveals the presence of RTN signals with anomalous characteristics (aRTN) besides the conventional two-level and multi-level RTN. These aRTN signals display more than two levels but strongly differ from multi-level RTN signals. Indeed, despite both the aRTN and the multi-level RTN signals are characterized by multiple discrete current levels, the aRTN cannot be represented by a superposition of *independent* two-level RTN fluctuations, as opposite to the multi-level RTN. Figure 2(a) shows an example of aRTN: the signal, which displays three discrete current levels, consists of two RTN components (each component is a two-level RTN fluctuation), i.e. a fast and a slow one, Fig. 2(a). The main difference with a standard multi-level RTN fluctuation is that in this case the fast RTN occurs only when the slow RTN

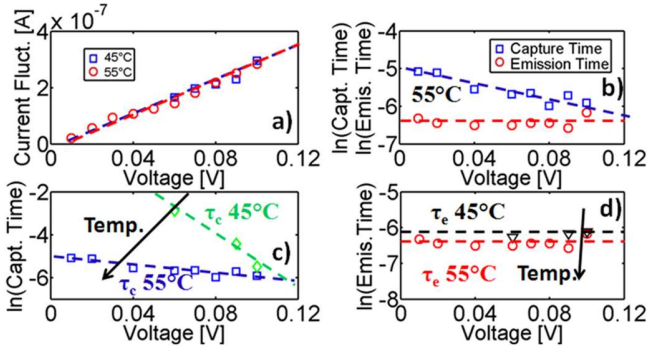


Figure 3. Fast RTN fluctuation statistical characteristics (both experimental – symbols – and fitting – dashed lines). (a) The amplitude of fluctuation is reported vs. voltage at different temperatures. (b) Capture and emission times vs. voltage at 55°C. (c) Capture and (d) emission times vs. voltage at different temperature. The RTN behavior is consistent with the prediction of TAT theory.

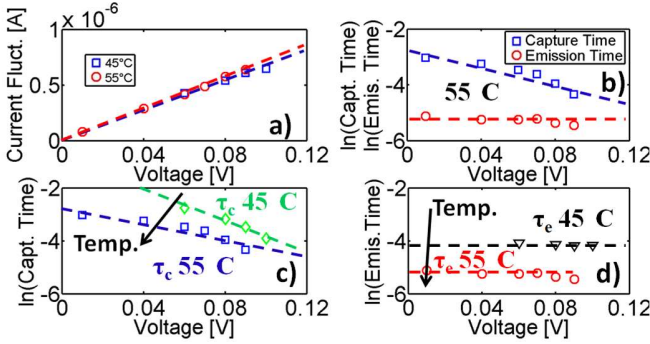


Figure 4. Slow RTN fluctuation statistical characteristics (both experimental – symbols – and fitting – dashed lines). (a) The amplitude of fluctuation is reported vs. voltage at different temperatures. (b) Capture and emission times vs. voltage at 55°C. (c) Capture and (d) emission times vs. voltage at different temperature. The RTN behavior is consistent with the prediction of TAT theory.

component is in the high current state, Fig. 2(b,c). This impedes describing aRTN as a superposition of *independent* two-level fluctuations. The straight application of the FHMM data analysis (or any other technique currently used to analyze RTN signal properties) to the signal as in Fig. 2(a) leads to equivocal results. Indeed the portions of the I - t trace in Fig. 2(c) highlighted with violet rectangles would be incorrectly considered in the estimation of the average emission time of the fast RTN component, resulting in an inaccurate evaluation. Contrariwise, aRTN signals can be described in terms of the superposition of *correlated* two-level fluctuations, as shown in Fig. 2(b,c). Indeed, the behavior of the fast component is directly influenced by the state of the slow one; green and violet rectangles in Fig. 2(b,c). So, it is necessary to consider the correlation between the two RTN components when estimating the characteristics of the fast RTN component. As such, in order to accurately extract the characteristics of the fast and slow components of the aRTN, we separately analyze each portion of the experimental I -time traces where the slow RTN fluctuation is in the high-current state. By carefully considering the correlation effect, we exploit advanced data analysis based on the FHMM [12-13] to derive the statistical characteristics (ΔI , τ_c , τ_e – see Fig. 2(b)) of both the fast and the slow RTN component. In this work we analyze the aRTN characteristics

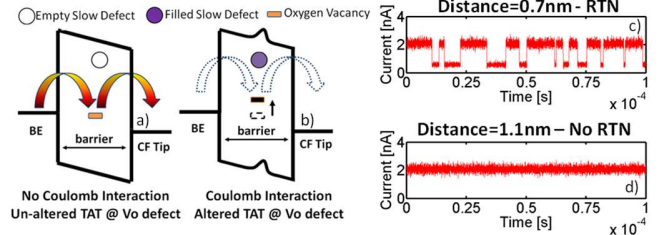


Figure 5. (a-b) Schematic illustration of the Coulomb blockade effect. (a) The TAT charge transfer via a Vo defect (shown in the bandgap) when the close “slow” defect is empty. (b) The charge trapping at the slow defect in the proximity of the Vo alters the potential and the energy alignment, suppressing the TAT current via the Vo. (c-d) Kinetic Monte-Carlo simulations of RTN given by the interaction between an individual Vo driving current and a “slow” defect placed at different distances from the Vo, (c) 0.7 nm – showing RTN, and (d) 1.1 nm – too far to generate RTN. The superimposed white noise is due to the average effect of the very fast Vo capture and emission processes (TAT).

related to a single bit, Section II-B. A preliminary data analysis indicates that the operating conditions (e.g. current compliance, reset voltage) have an insignificant effect on the aRTN characteristics, though the complexity of measurements, data analysis, and physical interpretation, prevents drawing noteworthy conclusions, which is out of the scope of this paper.

The aRTN characterization was performed at different operating conditions, i.e. temperatures and bias voltages. The characteristics (ΔI , τ_c , τ_e) of the fast RTN component at 55°C are plotted vs. the applied voltage, V_{READ} , in Fig. 3. The amplitude of the fluctuation (ΔI) increases with V_{READ} , also at different temperatures. Capture time exponentially decreases with V_{READ} while emission time keeps constant, consistently with the predictions of the Trap-Assisted Tunneling (TAT) model which includes the electron-phonon interaction through the multi-phonon lattice relaxation mechanism [15], Fig. 3(b). In addition, capture and emission times fall with temperature Fig. 3(c,d), again consistently with the TAT theory. The same behavior is verified analyzing the slow component, Fig. 4.

IV. PHYSICAL INTERPRETATION

The RTN current fluctuations are measured on devices in HRS, which is associated with the presence of a dielectric barrier within the CF [10]. In this resistive state, the charge transport is dominated by TAT at positively charged O vacancy defects, Vo, within the barrier [15], and the two-level RTN in HRS was attributed to the random activation and deactivation of an individual Vo [5-6]. Multi-level RTN was described as the simultaneous (but independent) activation and deactivation of many individual O vacancy defects, which is consistent with multi-level RTN being the superposition of independent two-level fluctuations, Section III. In the following, we will present a self-consistent physical framework encompassing charge transport and RTN, which is then exploited to discuss the mechanisms potentially responsible for the observed aRTN.

A. Charge Transport and Conventional RTN

Positively charged oxygen vacancy defects, Vo^+ , are identified as the defect configuration assisting charge transport through the very fast transition ($\text{Vo}^+ + e^- \rightarrow \text{Vo}^0 \rightarrow \text{Vo}^+ + e^-$) [15]. RTN fluctuations have been ascribed to the sudden changes

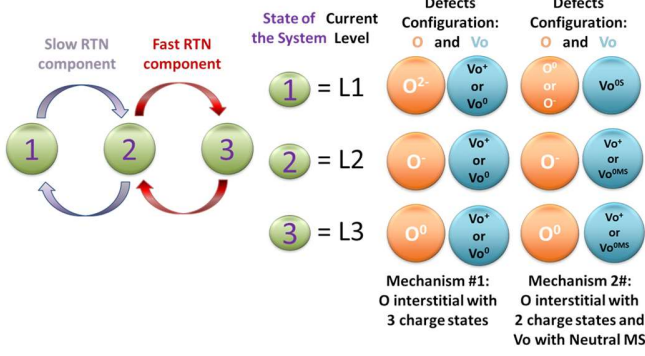


Figure 6. State-space representation of the aRTN. The three current levels in Fig. 2(a) are associated with three states of the system. The switching among these levels determines the aRTN. The defects configurations corresponding to the three states of the system are reported for the two different physical mechanisms which could lead to aRTN. Orange circles represent the O interstitial, while light blue circles represent the O vacancy.

	O vacancy	O interstitial
E_{REL}	0.7 eV	2.67 eV
E_T	2.2 ± 0.3 eV	2.3 ± 0.2 eV
σ_T	10^{-14} cm ²	$3 \cdot 10^{-16}$ cm ²
N_T	$2 \cdot 10^{21}$ cm ⁻³	10^{21} cm ⁻³
$E_{REL,MS}$	0.7 eV	-
$E_{REL,S}$	3 eV	-
$E_{REL,0}$	-	2.67 eV
$E_{REL,-1}$	-	3 eV

Table I. Parameters of the defect species considered in kMC simulations. E_{REL} is the relaxation energy, E_T the thermal ionization energy, σ_T the capture cross-section, N_T the density. $E_{REL,MS}$ and $E_{REL,S}$ are the relaxation energies related to the stable and metastable states of the Vo defect. $E_{REL,0}$ and $E_{REL,-1}$ are the relaxation energies related to the neutral-negative and negative-double negative transitions of the O interstitial. See [7, 9, 15-18].

in the current driven by an individual Vo, which could be due to the Coulomb blockade effect due to charge trapping and de-trapping at a defect of different nature in the Vo proximity, e.g. the neutral O interstitial [7, 16]. Indeed, charge trapping at the neutral O interstitial defect (i.e. $O^0 + e^- \rightarrow O^- \rightarrow O^0 + e^-$) perturbs the potential in its surroundings, potentially affecting the Vo trapping/de-trapping times. This directly influences the amount of TAT current the defect drives [16], as shown in Fig. 6(a-b). This mechanism allows explaining two-level fluctuations of the current driven by an individual Vo in the proximity of an O interstitial, depending on the O interstitial charge state (empty or filled), Fig. 5. Indeed, kinetic Monte-Carlo simulations show that RTN may naturally arise from the Coulomb interaction between a Vo defect driving current and an O interstitial defect (close to the TAT-supporting Vo) capturing and emitting charge, Fig. 5 (c-d). In this context, an individual two-level RTN fluctuation can be represented by a two-state system (i.e. the O interstitial can be either empty or filled with an electron). Accordingly, multi-level RTN arises from the superposition of several independent (i.e. non-interacting) two-state systems.

B. Anomalous RTN

The physical framework presented in Section IV-B, however, cannot be used as is to properly represent aRTN

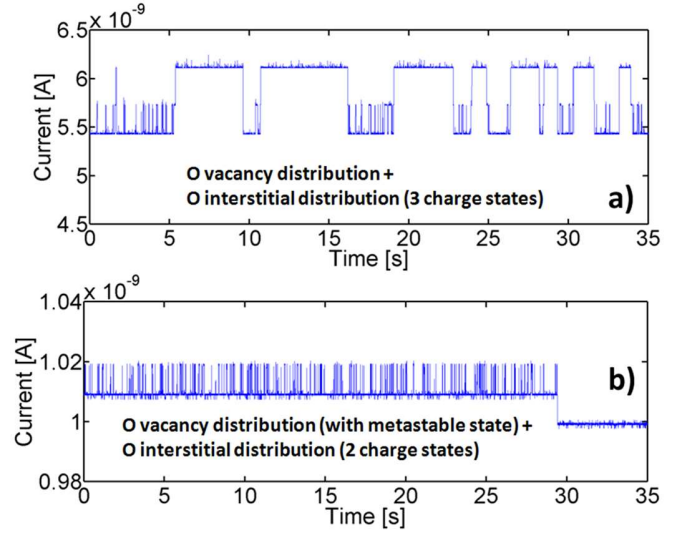


Figure 7. kMC simulations of a 5x5 nm² wide and 1.5nm thick HfO_x barrier considering a uniform distribution of positively charged Vo and neutral O interstitials. In (a) we consider the possibility for O interstitials to capture and emit charge both when neutral and negatively charged. In (b) we consider the presence of a neutral metastable state for the Vo.

signals due to the strong correlation effect between its components (fast and slow RTN in Fig. 2). In this respect, it is useful to characterize aRTN using a state-space representation, Fig. 6. The three discrete current levels in Fig. 2(a) are related to three different states of the system, possibly associated with different defect atomistic arrangements within the barrier. The switching dynamics heavily depends on the applied voltage and temperature, as confirmed by the trends shown in Figs. 3 and 4. These trends are in agreement with the predictions of the TAT theory [15], suggesting that also the switching among the three defect system states may result from charge trapping and emission phenomena as well, Fig. 6. It is beneficial to recall that, in HfO₂, defects may exist in different charge states (e.g. O interstitials exist in three charge states, from 0 to 2-) [17]. Each transition between charge states due to charge trapping and emission is characterized by precise values of thermal ionization energy and relaxation energy. These parameters determine the typical average capture and emission times and their dependence on the local voltage and temperature profiles. The positively charged O vacancies and neutral O interstitials are the defect configurations with the highest relative density in HfO₂ [17-18]. The three-state defect model required to explain the aRTN is developed allowing the O interstitials to be present also in the 2- charge state, e.g. $O^- + e^- \rightarrow O^{2-} \rightarrow O^- + e^-$, Fig. 6. The perturbation of the electric potential in the O interstitial surroundings, which include the close O vacancy site, depends on its actual charge state (which can be neutral, negative, or double negative). This threefold change in the potential affects the current driven by the Vo to three different extents. In order to verify whether this option could effectively explain the experimental aRTN characteristics, we use physics-based kMC simulations including the possibility for the defects to be in more than two charge states. Simulations are performed by considering a 5nm diameter and 1.5nm thick HfO₂ barrier. The details of the defects parameters used in the simulations are reported in Tab. I. Simulations include two distributions of

defects (Vo and O interstitials), properly considering the Coulomb interaction between the defects, and the possibility for O interstitials to capture and emit charge in both the neutral ($O^0 + e^- \rightarrow O^- \rightarrow O^0 + e^-$) and the negative state ($O^- + e^- \rightarrow O^{2-} \rightarrow O^- + e^-$) [17-18]. Results in Fig. 7(a) show that a correlated three-level fluctuation can be achieved, confirming that Coulomb potential perturbations due to multiple electron trapping at O interstitials can trigger aRTN. Notably, in the proposed scenario, the $1 \rightarrow 3$ state transition in Fig. 6 can only occur through the state #2, except considering the extremely rare double tunneling.

C. Metastable States

An alternative mechanism which could cause sharp changes in the current driven by a Vo, so possibly contributing to aRTN, rely on the existence of metastable states for Vo defects [7]. Metastable defect configurations have been used to explain long (up to 10-100s) capture and emission times in two-level RTN current fluctuation in several material systems [7]. Vo with metastable states (corresponding to different arrangement of the electrons across the atoms surrounding the defect) have recently been proposed in the literature to explain RTN. The theory predicts the existence of two different states associated with the same charge state: one metastable (fast) and one stable (slow). If, upon electron trapping, the defect is in its metastable state, the charge carrier will be quickly emitted: the time constant of the process is very small, and the electron being successively emitted can contribute to charge transport, Fig. 8. Conversely, if upon charge trapping the defect reaches its stable state (which requires overcoming a thermal barrier, Fig. 8), the time constant for the ensuing emission process is sufficiently large. This holds the electron at the defect site for a relatively long time, with the defect being temporarily unavailable to assist charge transport (until the system overcomes again the thermal barrier getting into the metastable state). Metastable states, proposed to explain two-level RTN, may also play a role in aRTN. In this framework, the lowest current level in Figs. 2 and 6 is associated with Vo in its positive stable state, i.e. Vo does not assist the TAT charge transport. As soon as the Vo transits to the positive metastable state, it can quickly capture an electron and get to the neutral charge state. The TAT charge transport is now supported (through the neutral \rightarrow positive metastable \rightarrow neutral transition), explaining the current in the state #3. In this scenario, the Coulomb interaction between Vo and the potential perturbation caused by a charge trapped at a close O interstitial, may affect the current driven by the Vo, causing the fast RTN fluctuation, Fig. 6. The electron capture/emission at the O interstitial affects the Vo energy alignment with the Fermi level, hence the current driven by the Vo. This possibility is confirmed by kMC simulations in Fig. 7(b), which include distributions of both positively charged Vo defects with a positive metastable state and neutral O interstitials: a correlated three-level fluctuation is correctly simulated. In this framework, the $1 \rightarrow 3$ state transition in Fig. 6 can occur directly, without passing via the state #2. It is worth noting that the parameters ruling the charge state transitions of defects in HfO_2 (thermal ionization and relaxation energies) are known from ab-initio calculations only for some defect species, and are typically calculated by considering isolated defects [17-18]. Similarly, the existence of metastable states for the Vo defects in HfO_2 is still to be demonstrated,

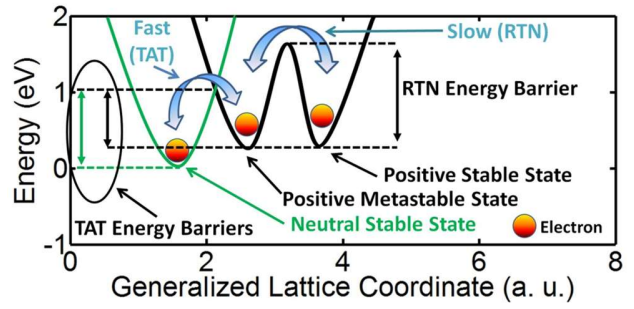


Figure 8. Generalized configuration coordination diagram illustrating the metastable states for the Vo defect explaining RTN: the TAT current involves the transition between the neutral and the positive metastable state of the Vo; the RTN fluctuations are generated by the transition of the positive metastable state into a stable configuration, temporarily inhibiting the TAT charge transport and causing RTN.

demanding further efforts to identify the dominant mechanism and defects configuration.

V. TEMPORARY PHENOMENA: DEFECTS DIFFUSION AND ELECTROSTATIC INTERACTIONS

The physical framework developed in Section IV constitutes a comprehensive setting to explore the physical causes of complex features of RTN signals found in these devices. This framework is now exploited to investigate temporary phenomena related to RTN. Indeed, besides two-level, multi-level, and anomalous RTN current fluctuations, several experimental observations [7, 20-23] underlined the existence of other temporary phenomena somehow related to RTN. Coarsely, we can classify these phenomena as follows:

1. Temporary RTN (tRTN) – a two-level RTN fluctuation randomly appearing and disappearing during RTN measurements. It differs from aRTN since it shows no correlation with additional two-level RTN fluctuations (components), Fig. 9.
2. Mutant RTN (mRTN) – a two-level RTN fluctuation which changes its statistical characteristics (i.e. capture and emission times, amplitude) for a given time (randomly distributed) before coming back to the original RTN signal. The phenomenon can be iterative, Fig. 10.

To properly investigate these phenomena it is mandatory to consider all the mechanisms occurring in the device in operating conditions. Hence, we have to include not only the mechanisms responsible for charge transport and its alterations (e.g. RTN), but also the mechanism responsible for structural modifications, i.e. defects generation/recombination, and drift/diffusion. These phenomena all play vital roles in the device switching [24]: the CF formation/restoration during the forming/set operations has been shown to be due to defects (Vo and O interstitial) generation and diffusion [9, 19], while the CF rupture during reset occurs due to O interstitials drift and their recombination with Vo defects constituting the CF [9]. To explain temporary phenomena like tRTN and mRTN, we must analyze their peculiar features. Figure 9(a) reports the tRTN as measured on an RRAM device in HRS in reading conditions.

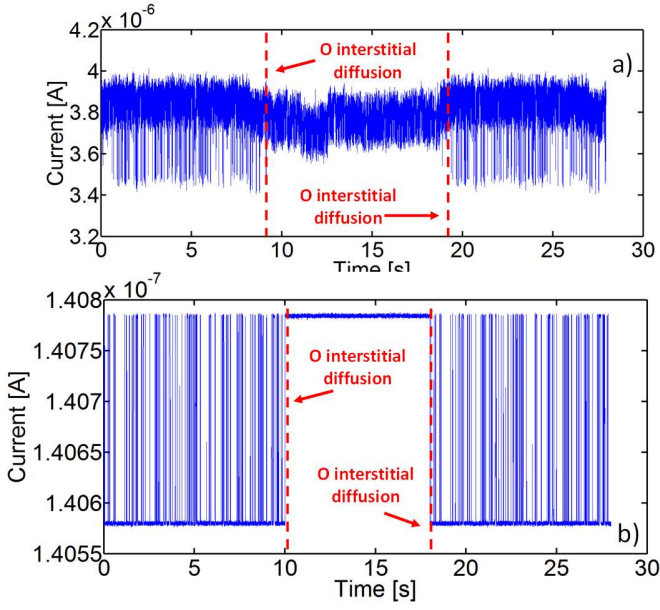


Figure 9. (a) Experimental tRTN measured in an RRAM device in HRS at $V_{\text{READ}}=60\text{mV}$ and $T=55^\circ\text{C}$. A two-level RTN fluctuation is switched off at $t \approx 9\text{s}$ to appear again at $t \approx 18\text{s}$ with the same characteristics (capture and emission times). (b) kMC simulations of a $5 \times 5 \text{ nm}^2$ wide and 1.0nm thick HfO_x barrier with 4 Vo defects randomly placed in the middle of the barrier and a neutral O interstitial defect close to them. Simulations include the O interstitial diffusion and reproduce the observed tRTN characteristics.

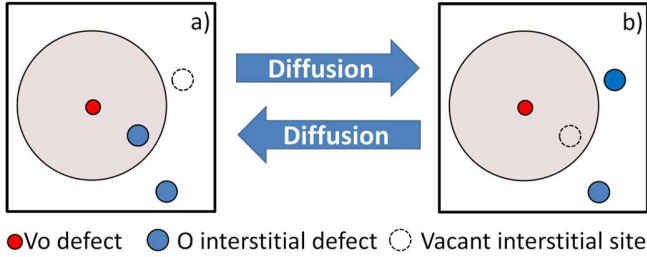


Figure 10. Schematic depiction of a possible diffusion scenario leading to tRTN. The Vo defects are the red spheres and the light-red region around them is the zone in which an O interstitial (blue spheres) must be for the Coulomb interaction between them to be significant (hence trigger RTN). (a) A Vo defect assists the TAT and its Coulomb interaction with an O interstitial generates RTN. (b) The O interstitial diffuses in a close available interstitial site far from the Vo , temporarily stopping the RTN. The mechanism of O interstitials drift/diffusion is responsible for the switching between the two atomistic arrangements.

This signal is characterized by a dominant two-level RTN fluctuation from the beginning of the measurement until $t \approx 9\text{s}$. Then, this two-level RTN fluctuation is switched off at $t \approx 9\text{s}$ to appear again at $t \approx 18\text{s}$. The measurement last until $t \approx 28\text{s}$, with this newborn fluctuation still being active, Fig. 9(a). Interestingly, when this tRTN fluctuation is visible (i.e. between $t=0\text{s}$ and $t \approx 9\text{s}$, but also between $t \approx 18\text{s}$ and $t \approx 28\text{s}$) it always shows the same statistical characteristics (ΔI , capture and emission times). In order to self-consistently explain tRTN, we must include in the proposed physical picture also defects drift-diffusion. Notably, this mechanism must be considered also in reading conditions (i.e. $V_{\text{READ}} \approx 100\text{mV}$). Indeed, when in HRS, the device exhibits a dielectric barrier having a typical thickness around 1nm which corresponds to a reading

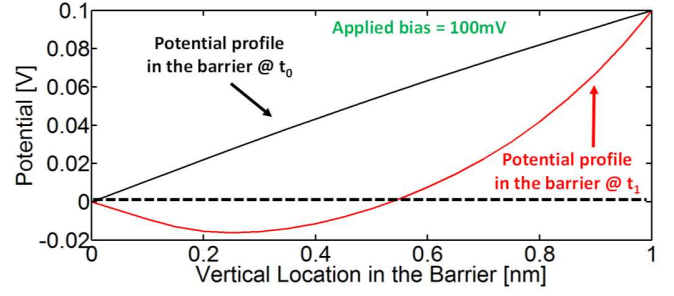


Figure 11. Simulated potential along the vertical direction (passing through the center of the device) profile in a $5 \times 5 \text{ nm}^2$ wide and 1.0nm thick HfO_x barrier at two different instants of time. Charge trapping and de-trapping at defects in the oxide may severely distort the potential profile, which shows significant variations over time.

conditions electric field $E_{\text{READ}} \approx 1\text{MV/cm}$. This value is comparable to the electric field which causes the migration of the O interstitials during the reset operation [25], which implies that diffusion of O interstitial defects also occurs in the barrier in reading conditions. Conversely, Vo diffusion in HfO_2 has been shown to be way less effective [17, 18, 26].

In the following we show how considering both the Coulomb interaction among charged defects (see Section IV) and the possible O interstitial diffusion allows reproducing both tRTN and mRTN. From Section IV, we recall that a two-level RTN fluctuation is the result of the Coulomb interaction between a Vo defect (or a group of Vo defects) assisting TAT charge transport and an O interstitial defect in its (their) proximity [16, 27]. The statistical characteristics of the RTN (ΔI , τ_c , τ_e) are strictly dependent on the position and energy of the Vo defects assisting the current (ΔI) and of the O interstitial (τ_c , τ_e) [15]. Clearly, if the physical and/or energetic location of the O interstitial changes over time (e.g. due to the diffusion mechanism) we expect a corresponding change in the RTN statistical properties (τ_c , τ_e). The characteristics of the tRTN trace in Fig. 9(a) suggest that, if diffusion is responsible for the observed behavior, the O interstitial should diffuse away from its original location at $t \approx 9\text{s}$, moving in an adjacent interstitial site hence changing its physical/energetic location, as shown in Fig. 10. This shift radically changes the O interstitial capture and emission dynamics, resulting in a significant variation of the RTN properties (τ_c , τ_e). The amount of variation of the RTN properties due to the O interstitial diffusion strongly depends on the local arrangement of the defects and on the location of available interstitial sites. For instance, if the new physical location of the O interstitial happens to be very close to the original one, then the change in the RTN properties will be correspondingly small. In the opposite scenario, the change in the RTN properties may be so severe that the new τ_c and τ_e could easily get larger (smaller) than the measurement (sampling) time, which causes the RTN interruption in the measurement. Moreover, if the new location of the O interstitial is too far from the Vo defect assisting the TAT current, the RTN fluctuation will cease existing due to the heavy reduction in the Coulomb interaction [16, 27], Section IV. This is the case shown in Fig. 9(a), in which the RTN fluctuation disappears at $t \approx 9\text{s}$. Nevertheless at $t \approx 18\text{s}$ the RTN fluctuation reappears showing the original statistical properties (τ_c , τ_e). In this scenario the diffusion of the O interstitial at $t \approx 9\text{s}$

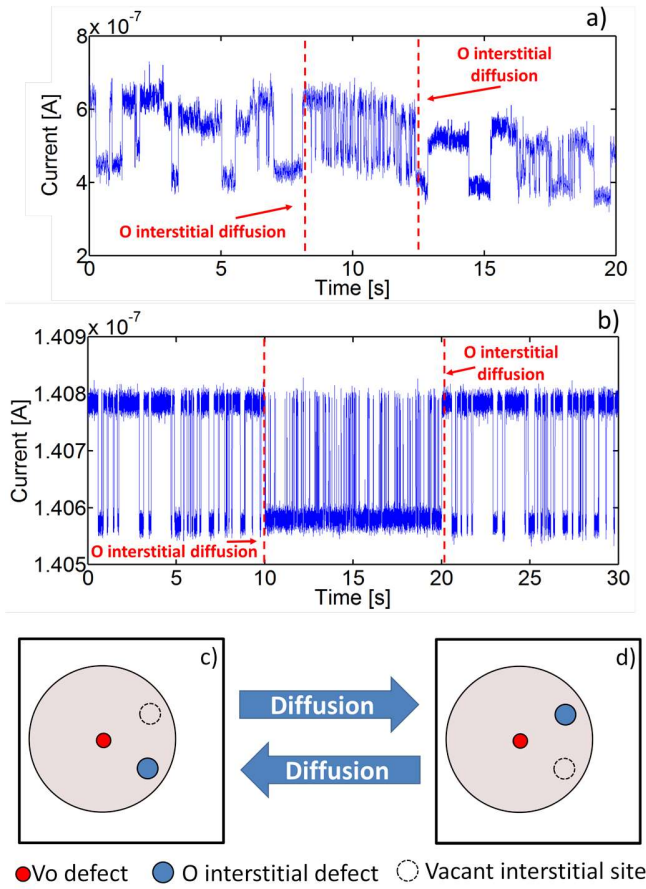


Figure 12. (a) Experimental mRTN measured in an RRAM device in HRS at $V_{\text{READ}}=80\text{mV}$ and $T=45^\circ\text{C}$. A two-level RTN fluctuation temporarily changes its capture and emission times due to O interstitial diffusion. (b) kMC simulations of a $5\times 5\text{ nm}^2$ wide and 1.0nm thick HfO_x barrier with 4 Vo defects in the middle of the barrier and a neutral O interstitial defect close to them. Simulations include the O interstitial diffusion mechanism and reproduce the observed mRTN characteristics. (c-d) Schematic depiction of a possible diffusion scenario leading to mRTN. The Vo defects are the red spheres and the light-red region around them is the zone in which an O interstitial (blue spheres) must be for the Coulomb interaction between them to be significant (hence trigger RTN). (c) A Vo defect assists the TAT and its Coulomb interaction with an O interstitial generates RTN. (d) The O interstitial diffuses in an available interstitial site close to the Vo, temporarily altering the RTN characteristics. The mechanism of O interstitials drift/diffusion is responsible for the switching between the two atomistic arrangements.

leaves behind an available interstitial site which is filled by another O interstitial at $t\approx 18\text{s}$, Fig. 10. This new atomistic configuration is naturally compatible with the re-appearance of RTN with the original statistical characteristics.

Interestingly, at low applied voltages (i.e. reading conditions) the diffusion paths followed by O interstitial defects are not preferentially determined by the direction of the applied electric field. Conversely, their diffusion motion appears to be disordered, since the potential profile in the device is severely distorted by trapped charges. This is elucidated in Fig. 11, in which the simulated potential profile in the device along the vertical direction at different times is reported. Defects charging and discharging heavily influence

the potential profile, which significantly varies over time. Notably, the potential can also revert its polarity at some locations along the vertical location (it becomes negative as shown in Fig. 11) compared to the applied voltage, which is positive, suggesting that the O interstitial diffusion paths may be unexpectedly driven by local changes in the electrical field especially in the middle of the barrier, Fig. 11. The analysis of the diffusion paths is further complicated by the effect of temperature inside the device, which can locally increase as a results of the heterogeneous power dissipation at active Vo defects assisting TAT [9, 15-16, 24, 27]. Moreover, the activation and deactivation of TAT-supporting defects due to RTN confer temporary attributes to these local temperature variations, which further complicates the overall picture. These variations of the local temperature profile can in turn affect O ion/vacancy diffusion processes, influencing the dynamics of temporary phenomena. Strikingly, considering the diffusion mechanism in simulations with an activation energy for O interstitial diffusion $E_D\approx 0.3\text{eV}$ [26], allows reproducing tRTN, Fig. 9(b).

Interestingly, the same physics-based simulation framework used to describe tRTN can be adopted to explain also mRTN. Indeed, if an O ion causing RTN (hence close enough to a TAT-supporting Vo defect) only slightly changes its position as a result of interstitial diffusion (without changing the atomic configuration of the defect), Fig. 12(c-d), then the change in the RTN properties will be correspondingly small. This scenario corresponds to the presence of mRTN fluctuations which are correctly reproduced in simulations, Fig. 12(b). In this case, we considered for mRTN simulations an atomic configurations, i.e. 4 Vo defects and an individual O interstitial defect randomly placed in 1nm -thick barrier, similar to the one which allows reproducing the tRTN fluctuations shown in Fig. 9. The differences between the two cases are just dictated by the random positions of both the O vacancies and the ion, confirming the stochastic nature of the microscopic processes governing tRTN and mRTN phenomena, involving drift/diffusion and charge trapping/de-trapping.

It is interesting to note that despite small differences in the initial O vacancy-ion configuration, the random diffusion path of the O interstitial, as compared to the positions of the Vo defects, can result in either tRTN or mRTN. Thus, tRTN and mRTN are simply different evidences of the same physical phenomenon, which is due to the complex interplay among the local modification of the electrical potential (due to both charge trapping and ion/vacancy diffusion), the local temperature increase, the charge transport mechanisms (drift/diffusion, TAT), and the diffusion of O interstitial ions.

Notably, these phenomena cannot be explained by random field-assisted generation and recombination of defect pairs (i.e. Hf-O bond breakage) [9, 19]. Indeed, in this scenario, the appearance of a new RTN fluctuation would be related to the generation of a Vo defect and an O interstitial. The newly created Vo could start assisting TAT current and its activation and de-activation (either due to the Coulomb interaction with the newly created O interstitial or to the possible Vo metastable states - see Section IV) would result in the observed new RTN fluctuation. Similarly, the disappearance of a two-level RTN fluctuation during a measurement could be related to defects

recombination. However, this would imply the recombination of a defect pair (which have a definite position in the oxide layer) at a given instant of time (e.g. ≈ 10 s in Fig. 9(a)) and the ensuing generation of another defect pair (e.g. at ≈ 18 s in Fig. 9(a)) at the same exact location. This is a very unlikely scenario as defects generation is a completely stochastic mechanism [19] (at least in reading conditions, at which the temperature in the device is uniform). So, even though defects generation and recombination occur in the barrier, they cannot be responsible for tRTN and mRTN phenomena.

Interestingly, temporary RTN phenomena were also recently observed in SiO₂ and SiON pMOSFETs [28-29]. In [28], the authors consider these phenomena the result of some "defect volatility": the RTN signals appear and disappear, resembling tRTN. This defect volatility, observed under a variety of conditions, was cautiously attributed to possible interactions between oxygen vacancy defects and hydrogen atoms/molecules, which interact with Vo defects causing their temporary passivation. Moreover, "defect transformation" resulting in the sudden change of RTN timing characteristics resembling mRTN has also been reported, and tentatively attributed to the flexibility of the SiO₂ network easily allowing local rearrangements at defect sites [28-29].

In principle, both the mechanisms proposed in [28-29] and the ones investigated in this work could be involved in RTN and related phenomena. Potentially, their relative impact on the observed RTN could change when different materials and defects typologies are considered: a deeper understanding of the defects nature and properties could help to clarify aspects related to these different but extremely interesting physical playgrounds.

To conclude, we summarize here the results shown in this work, which have important similarities with those observed in other material systems:

1. The characterization of RTN and related phenomena must be performed carefully, consider also possible correlation among superimposed RTN components (aRTN). A reliable extraction of the RTN statistical parameters, crucial to the understanding of the underlying physical phenomena, is possible only if careful measurements and advanced data analysis are performed together [30-31].
2. The electrostatic interactions among charged defects play a crucial role in RTN and related phenomena, as they alter the local profile of electrical potential, which stochastically affects charge trapping, charge transport, interstitial ion drift and diffusion.
3. Achieving a self-consistent and inclusive understanding of the different phenomena occurring in these devices and in similar systems requires adopting a comprehensive physical framework. The latter must simultaneously consider all the above physical mechanisms and, most importantly, their complex interplay which has been shown to determine experimentally observed phenomena like tRTN and mRTN. This characteristic dramatically complicates the analysis and characterization of such phenomena and simultaneously show that neglecting the effects of this complex interplay results in a misleading (at

least) and potentially wrong (at most) interpretation of the experimental results.

VI. CONCLUSIONS

In this work we explored the characteristics of aRTN and temporary noise phenomena (i.e. tRTN and mRTN) in RRAM devices. Systematic experiments, refined data analysis techniques, and physics-based simulations were exploited to understand the possible mechanisms responsible for aRTN. They are found to rely on the possibility for defects in HfO₂ to have many charge states. Both the coulomb interaction between different defect species (i.e. Vo and O interstitials) and the existence of Vo with metastable states may explain the aRTN characteristics, pointing out the central role played by oxygen in TMO-based RRAM devices. The same physical framework, which encapsulates all the fundamental mechanisms describing charge transport and its alterations, as well as the structural modifications occurring at the nanoscale, is successfully used to predict other noise-related phenomena like tRTN and mRTN. The results shed new light on these phenomena and underline the essential role played by the Coulomb electrostatic interactions among trapped charges at defect sites. Moreover, the whole work highlights how the analysis of these complex phenomena must be performed exploiting a comprehensive physical framework simultaneously considering a wide variety of mechanisms and, most importantly, their complex interplay.

REFERENCES

- [1] Y.-S. Chen et al., "Highly scalable hafnium oxide memory with improvements of resistive distribution and read disturb immunity", Proceedings of the IEEE International Electron Devices Meeting (IEDM), pp.1-4, 7-9 Dec. 2009.
- [2] X. P. Wang et al., "Highly compact 1T-1R architecture (4F² footprint) involving fully CMOS compatible vertical GAA nanopillar transistors and oxide-based RRAM cells exhibiting excellent NVM properties and ultra-low power operation", IEEE International Electron Devices Meeting (IEDM) 2012, pp.20.6.1,20.6.4, 10-13 Dec. 2012.
- [3] W. Ma et al., "Multilevel resistive switching in HfO_x/TiO_x/HfO_x/TiO_x multilayer-based RRAM with high reliability", Proceedings of the 12th IEEE International Conference on Solid-State and Integrated Circuit Technology (ICSICT), pp.1-3, 28-31 Oct. 2014.
- [4] N. Raghavan et al., "RTN insight to filamentary instability and disturb immunity in ultra-low power switching HfO_x and AlO_x RRAM", Symposium on VLSI Technology (VLSIT) 2013, pp.T164-T165, 11-13 June 2013.
- [5] F. M. Puglisi et al., "Random Telegraph Signal noise properties of HfO_x RRAM in high resistive state", Proceedings of the European Solid-State Device Research Conference (ESSDERC) 2012, pp.274,277, 17-21 Sept. 2012.
- [6] D. Veksler et al., "Random telegraph noise (RTN) in scaled RRAM devices", Proceedings of the IEEE International Reliability Physics Symposium (IRPS), pp.MY.10.1-MY.10.4, 14-18 April 2013.
- [7] T. Grassler, "Stochastic charge trapping in oxides: From random telegraph noise to bias temperature instabilities", Microelectronics Reliability vol. 52(1), pp. 39-70, 2012.
- [8] K. G. Young-Fisher et al., "Leakage Current-Forming Voltage Relation and Oxygen Gettering in HfO_x RRAM Devices," in Electron Device Letters, IEEE, vol.34, no.6, pp.750-752, June 2013.
- [9] G. Bersuker et al., "Metal oxide resistive memory switching mechanism based on conductive filament properties", Journal of

- Applied Physics vol.110, no.12, pp.124518,124518-12, Dec. 2011.
- [10] F. M. Puglisi et al., "An Empirical Model for RRAM Resistance in Low- and High-Resistance States," IEEE Electron Device Letters, vol.34, no.3, pp.387,389, March 2013.
 - [11] F. M. Puglisi, P. Pavan, A. Padovani, L. Larcher, "A compact model of hafnium-oxide-based resistive random access memory", Proceedings of IEEE International Conference on IC Design & Technology (ICICDT) 2013, pp.85,88, 29-31 May 2013.
 - [12] F. M. Puglisi, P. Pavan, "RTN analysis with FHMM as a tool for multi-trap characterization in HfO_x RRAM", Proceedings of IEEE International Conference on Electron Devices and Solid-State Circuits (EDSSC) 2013, pp.1-2, 3-5 June 2013.
 - [13] F. M. Puglisi, P. Pavan, "Factorial Hidden Markov Model analysis of Random Telegraph Noise in Resistive Random Access Memories", ECTI Transactions on Electrical Engineering, Electronics, and Communications, vol. 12, no.1, pp. 24-29, 2014.
 - [14] <http://www.mdlab-software.com>
 - [15] L. Vandelli et al., "A Physical Model of the Temperature Dependence of the Current Through SiO₂/HfO₂ Stacks", IEEE Transactions on Electron Devices, vol.58, no.9, pp.2878-2887, Sept. 2011.
 - [16] F. M. Puglisi et al., "A microscopic physical description of RTN current fluctuations in HfO_x RRAM", Proceedings of the IEEE International Reliability Physics Symposium (IRPS), pp. 5B.5.1-5B.5.6, 19-23 April 2015.
 - [17] A. S. Foster et al., "Vacancy and interstitial defects in hafnia", Phys. Rev. B, Condens. Matter, vol. 65, no. 17, p. 1744 117, May 2002.
 - [18] D. Muñoz Ramo et al., "Spectroscopic properties of oxygen vacancies in monoclinic HfO₂ calculated with periodic and embedded cluster density functional theory", Phys. Rev. B, Condens. Matter, vol. 75, no. 20, p. 205 336, May 2007.
 - [19] J. McPherson et al., "Thermochemical description of dielectric breakdown in high dielectric constant materials", Appl. Phys. Lett. 82, 2121, 2003.
 - [20] F. M. Puglisi, L. Larcher, A. Padovani, P. Pavan, "Characterization of anomalous Random Telegraph Noise in Resistive Random Access Memory", Proceedings of the 45th European Solid State Device Research Conference (ESSDERC), pp.270-273, 14-18 Sept. 2015.
 - [21] S. Ambrogio, S. Balatti, V. McCaffrey, D. Wang, D. Ielmini, "Impact of low-frequency noise on read distributions of resistive switching memory (RRAM)", Proceedings of the IEEE International Electron Devices Meeting (IEDM), pp.14.4.1-14.4.4, 15-17 Dec. 2014.
 - [22] S.-C.H. Chen et al., "New observations on the regular and irregular noise behavior in a resistance random access memory", IEEE International Integrated Reliability Workshop Final Report (IIRW), pp.94-98, 12-16 Oct. 2014.
 - [23] Y. J. Huang et al., "The physical insights into an abnormal erratic behavior in the resistance random access memory", Proc. of the IEEE International Reliability Physics Symposium (IRPS), pp.MY.3.1-MY.3.4, 14-18 April 2013.
 - [24] L. Vandelli et al., "Comprehensive physical modeling of forming and switching operations in HfO₂ RRAM devices", Proceedings of the IEEE International Electron Devices Meeting (IEDM), pp.17.5.1-17.5.4, 5-7 Dec. 2011.
 - [25] S. Yu, H.-S. P. Wong, "A Phenomenological Model for the Reset Mechanism of Metal Oxide RRAM", IEEE Electron Device Letters, vol.31, no.12, pp.1455,1457, Dec. 2010.
 - [26] A. S. Foster, A. L. Shluger, and R. M. Nieminen, "Mechanism of Interstitial Oxygen Diffusion in Hafnia", Phys. Rev. Lett. 89, 225901.
 - [27] F. M. Puglisi, L. Larcher, A. Padovani, P. Pavan, "A Complete Statistical Investigation of RTN in HfO₂-Based RRAM in High Resistive State", IEEE Transactions on Electron Devices, vol.62, no.8, pp.2606-2613, Aug. 2015.
 - [28] T. Grasser et al., "On the volatility of oxide defects: Activation, deactivation, and transformation", Proc. of the IEEE International Reliability Physics Symposium (IRPS), pp.5A.3.1-5A.3.8, 19-23 April 2015.
 - [29] T. Grasser et al., "Hydrogen-related volatile defects as the possible cause for the recoverable component of NBTI", Proc. of the IEEE International Electron Devices Meeting (IEDM), pp.15.5.1-15.5.4, 9-11 Dec. 2013.
 - [30] G. Kapila and V. Reddy, "Impact of sampling rate on RTN time constant extraction and its implications on bias dependence and trap spectroscopy," IEEE Trans. Device Mater. Rel., vol. 14, no. 2, pp. 616–622, Jun. 2014.
 - [31] F. M. Puglisi, and P. Pavan, "Guidelines for a Reliable Analysis of Random Telegraph Noise in Electronic Devices", IEEE Trans. Instrum. Meas., in press. doi: 10.1109/TIM.2016.2518880